

Supporting Information:
**Mechanics under pressure of gold
nanoparticles supracrystals : the role
of the soft matrix**

July 5, 2022

1 Synthesis and characterization of the gold nanoparticles

The gold nanoparticles (NPs) have been synthesized using the Stucky method.¹ At the end of the reaction, the solvent is evaporated and ethanol is added to form a dark brown precipitate that is filtered off and washed with ethanol then dried. The NPs are then dispersed in oil. Organic solvents and the other chemicals were purchased from Sigma-Aldrich Co. and were used as received. The core diameter D_c has been measured by TEM (Fig. 1a) and SAXS (Fig. 1b) using NPs dilute suspensions in toluene: $D_c = 4.9$ nm with 8% polydispersity. TEM was performed at IMAGIF (I2BC CNRS, Gif s/Yvette, France) using a JEOL JEM-1400 microscope operating at 120 kV with a filament current of about 55 μ A. SAXS has been performed on the D2AM beamline at ESRF. The grafting density (5.2 nm^{-2}) has been determined by thermogravimetric analysis using the 6000@Perkin Elmer STA (Simultaneous Thermal Analyzer) performed on a batch of NPs similar to the one used in the pressure experiment.

¹Zheng N., Fan J. and Stucky G. D., J. Am. Chem. Soc., 128, 20, p 6550-6551,2006,doi: 10.1021/ja0604717

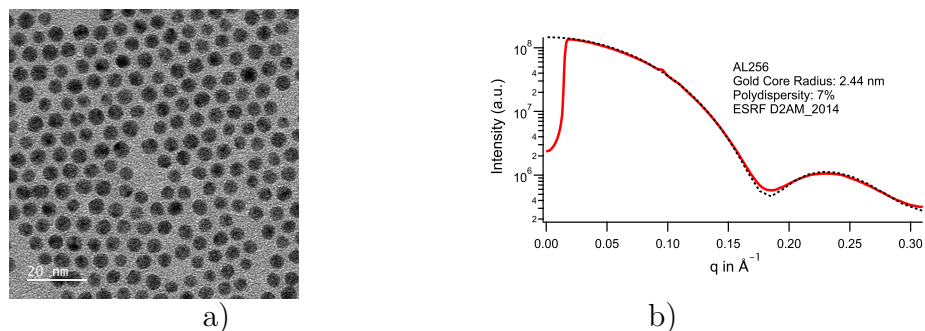


Figure 1: a) Nanoparticle TEM images b) SAXS pattern on a dilute (1 w%) nanoparticle suspension

2 Growth of the supracrystals and their imaging using MEB

To perform a controlled self-assembly process, the NPs are dispersed in a volatile oil like toluene or cyclohexane at an intermediate weight fraction (typically 15 wt%). The suspensions are then stirred and sonicated before being poured in cylindrical X-ray glass capillaries (diameter 1.5mm, WJM glas @) sealed at one end. The height of the capillaries is typically 10 cm, they are initially half-filled and kept vertically to allow slow evaporation of the solvent by the top at room temperature. After several days, supracrystals appear at the bottom of the capillaries and their structure is controlled by SAXS. When all the solvent is evaporated, the glass capillary is broken and large monodomains of supracrystals (few tenths of microns) can be extracted. These domains are then deposited into a diamond anvil cell.

Single domains with typical size of few tens of microns can be obtained as shown in Fig. 2. Scanning electron microscopy (FEG-SEM) images were performed at LPS, Orsay using a Zeiss SUPRA55VP/Gemini microscope. The imaging was performed under high vacuum at an accelerating voltage of 5 KV. Images were obtained from the backscattered electrons using the Everhart - Thornel Secondary Electron Detector (SE2) (Fig. 2a) and from the secondary electron signal using the High Efficiency InLens detector (Fig. 2b).

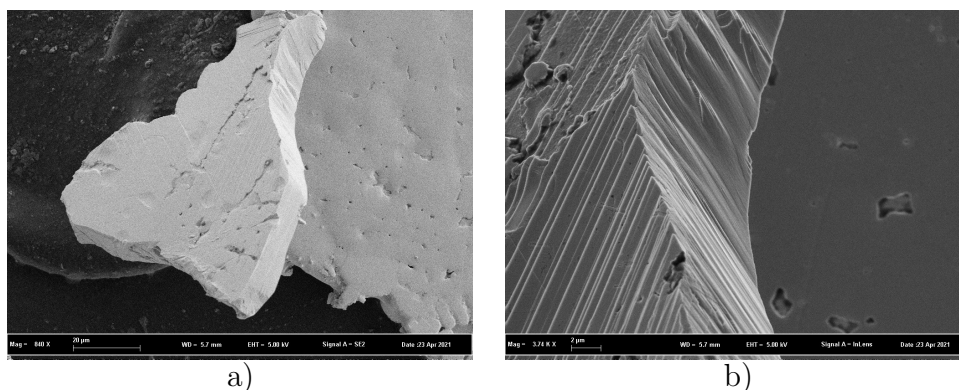


Figure 2: MEB images of a supracrystal (typical size $50 \mu\text{m}$), from the same batch as those placed in the pressure cell. The supracrystals have been grown by slow evaporation of a NP suspension in a volatile oil poured in a glass capillary.

3 Pressure Cell

To apply the pressure, membrane driven diamond anvil cells (DAC) were used, with $600\mu\text{m}$ diamonds culets. A CuBe gasket indented to 80 microns thickness and a $300\mu\text{m}$ -diameter hole was drilled. A $100\mu\text{m}$ piece of supracrystal was then placed in the hole, together with a ruby chip and Si oil as transmitting medium. The silicone oil is known to remain quasi-hydrostatic up to 10 GPa at room temperature ², within the range of this study. The standard ruby fluorescence technique ³ was used to monitor the pressure inside the sample chamber in the DAC. The ruby inside the DAC chamber was excited using a class 3b laser ($\lambda=405\text{nm}$). The fluorescence signal was transmitted to the spectrometer (HR4000 ocean optics; 0.47nm resolution) via an optical fiber that was fixed and not touched during the whole experiment, ensuring the same entrance condition of light on the spectrometer. The whole setup was inside the experimental hutch of Swing beam-line where the temperature is monitored and stable. The R1 line was fitted using a pseudo-voigt function combining Lorentzian and Gaussian functions

²Tateiwa N. and Haga Y., Review of Scientific Instruments, **80**, 12, p 1-9, 2009, doi:10.1063/1.3265992

³Chijioke A. D., Nellis, W. J., Soldatov, A. and Silvera I. F., Journal of Applied Physics **98**, 10, p 114905, 2005, doi: 10.1063/1.2135877

to maximize accuracy. The ruby fluorescence was first measured before applying pressure, ensuring the calibration of the initial wavelength at zero pressure for each ruby chip. The pressure was increased by finite steps, with real-time monitoring of the fit-determined pressure, with some delay to allow the pressure to stabilize. Pressure was measured before and after each SAXS measurement, with variation (typically 0.05 GPa at low pressure) well below estimated and reported uncertainty.

4 Diffraction pattern upon pressure

The supracrystal structure under pressure has been determined by SAXS. All results have been obtained during the Run 20201484 on the Swing beamline of the synchrotron Soleil (France). The energy of the x-ray beam was 16 keV, and its wavelength was 0.775 Å. The sample-detector distance was $D=0.519$ m and the size of the focused beam was typically 0.4mm (H)x0.1mm(V). The wave vector norm q is defined by $q = 4\pi \sin \theta / \lambda$ where 2θ is the angle between the scattered beam and the direct beam. The pixel detector (Eiger 4M, Dectris) is an assembly of several modules, with some gaps between them.

5 Indexation of the diffracted patterns of the supracrystal FCC structure.

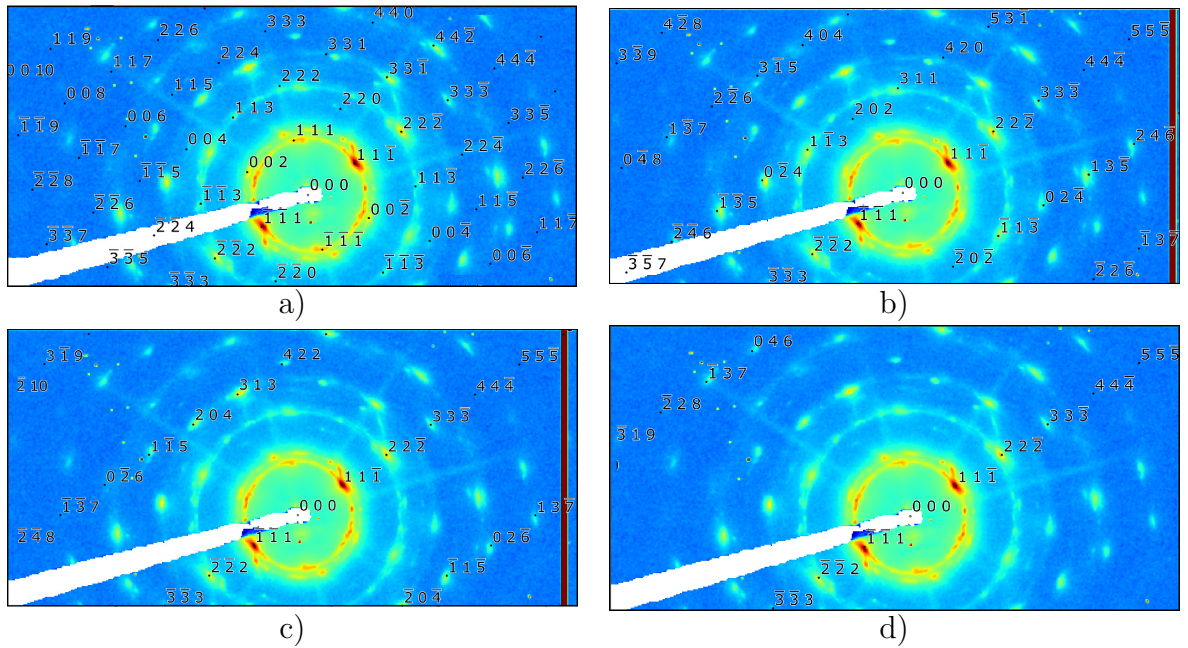


Figure 3: Indexation of the different domains observed at 0.2 GPa: a) domain 1: perpendicular to the $[1\bar{1}0]$ direction, b) domain 2: perpendicular to the $[\bar{2}30]$ direction c) domain 3: perpendicular to the $[\bar{1}21]$ direction, domain 4: perpendicular to the $[5\bar{3}1]$ direction

6 Determination of the bulk modulus: the different models

The behaviour and properties of earth materials at high pressure and temperatures have been described by different theoretical equation of state (EOS) $P(V)$. They are based on the interaction between atoms in solids. Several parameters are introduced: the volume at vanishing pressure V_0 , the bulk modulus at vanishing pressure B_0 and its derivative with respect to pressure B'_0 . These equation of state involve the variable $\eta = \left(\frac{V}{V_0}\right)^{1/3}$.

A largely used model leads to the Vinet ⁴ EOS expression:

$$P(V) = 3B_0 \left(\frac{1-\eta}{\eta^{2/3}} \right) \exp\left(\frac{3}{2}(B'_0-1)(1-\eta)\right) \quad (1)$$

Another model is the Murnaghan EOS, ⁵

$$V(P) = \frac{V_0}{(1 + P \frac{B'_0}{B_0})^{1/B'_0}} \quad (2)$$

Even if soft matter systems behave as classical solids, the interaction may be quite different. For polymeric and glass systems, J. Rault ⁶ has proposed another EOS based on three parameters V_0 , V^* and P^* . V^* is the limit volume at high pressure and P^* is related to the bulk modulus at vanishing pressure:

$$B_0 = P^* \frac{V_0}{V_0 - V^*}.$$

The EOS established by J. Rault is the following:

$$V - V^* = (V_0 - V^*) * \frac{1}{1 + P/P^*} \quad (3)$$

The bulk modulus at pressure P is

$$B(P) = P^* \left(1 + \frac{P}{P^*} \right)^2 \left(\frac{V^* + (V_0 - V^*) \left(1 + \frac{P}{P^*} \right)}{V_0 - V^*} \right) \quad (4)$$

One can deduce from this expression that:

$$B'_0 = \frac{V_0 + V^*}{V_0 - V^*}$$

⁴Vinet P., Smith J. R., Ferrante J. and Rose J. H., Phys. Rev. B, **35**, 4, pp 1945–1953, 1987, doi: 10.1103/PhysRevB.35.1945

⁵ Kumar M., Physica B: Condensed Matter, **212**, Issue 4, 1995, pp 391-394, doi.org/10.1016/0921-4526(95)00361-C.

⁶ Rault J., A universal modified van der Waals equation of state. Part I: Polymer and mineral glass formers, EPJE, **37**, p 113, 2014, doi=10.1140/epje/i2014-14113-3

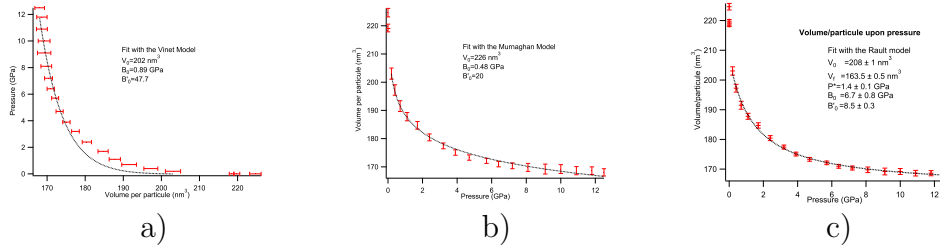


Figure 4: Comparison between the different EOS on the mechanical behavior of FCC supracrystal upon pressure: a) Vinet EOS b) Murnaghan EOS c) Rault EOS

7 Effet of the gold core modulus on the matrix bulk modulus

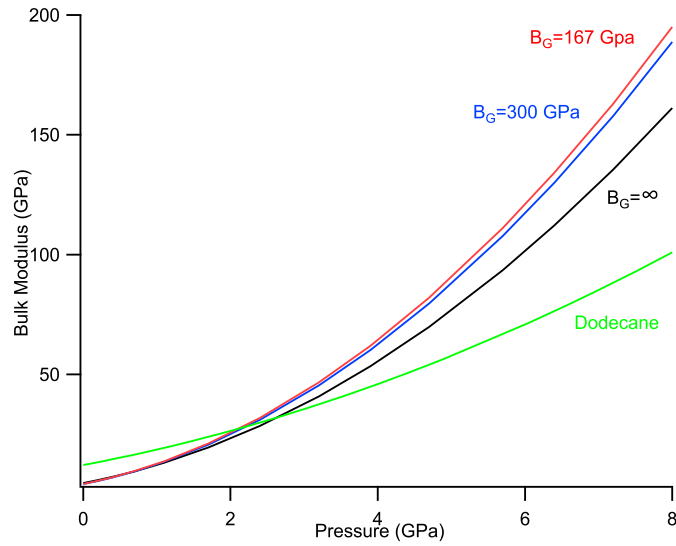


Figure 5: Effect of the gold core modulus on the matrix bulk modulus: $B_g = 167$ Gpa (bulk gold), $B_g = 300$ Gpa (estimation of the bulk modulus of a small gold core), $B_G = \infty$.

8 Diffraction patterns of dodecane under pressure

Dodecane crystallization appears above 0.3 GPa.

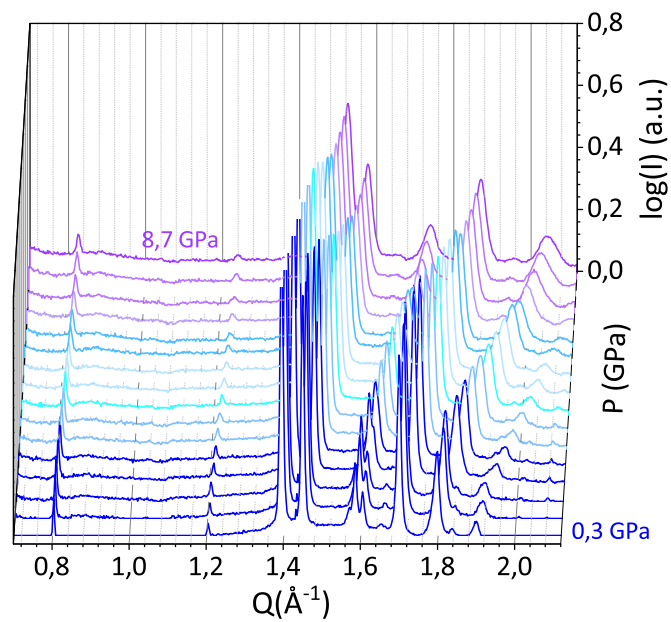


Figure 6: Diffraction pattern of dodecane under pressure: radial integration $I(Q)$

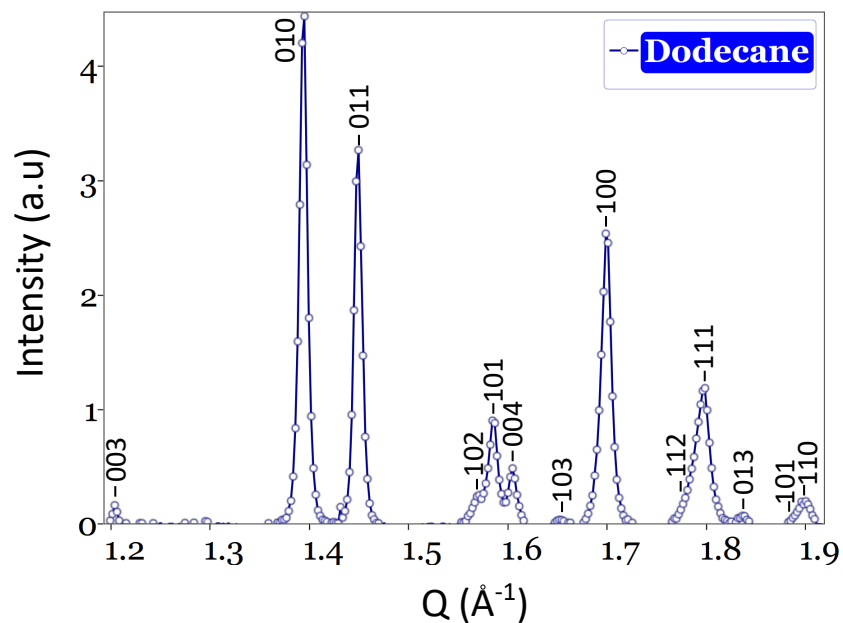


Figure 7: Expected diffraction pattern for a triclinic structure.

The unit cell of a triclinic system is described by 6 parameters: three lengths a , b and c and three angles α , β , γ . These parameters have been determined from the scattered patterns. The volume of the unit cell for this triclinic system is defined by:

$$V_{cell} = abc\sqrt{1 - \cos^2 \alpha - \cos^2 \beta - \cos^2 \gamma + 2 \cos \alpha \cos \beta \cos \gamma} \quad (5)$$

This volume is the volume per molecule since there is only one molecule per unit cell.

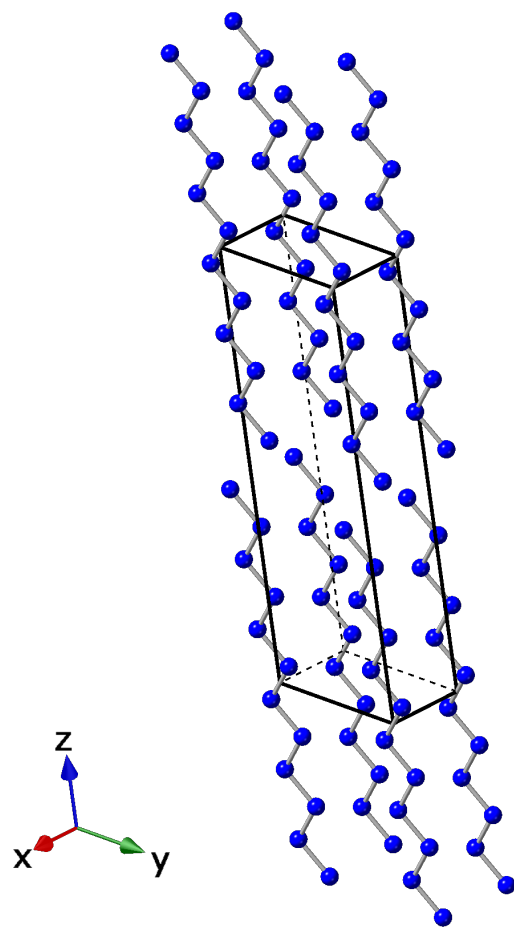


Figure 8: Dodecane molecule in the triclinic cell

P(Gpa)	a	b	c	α	β	γ	volume
0.00	4.193	4.697	17.17	1.451	1.149	1.285	296.11
0.30	4.190	4.698	17.15	1.452	1.152	1.285	295.85
0.35	4.149	4.670	17.05	1.454	1.161	1.288	290.84
0.54	4.116	4.618	17.08	1.451	1.151	1.287	284.56
0.69	4.082	4.586	17.01	1.450	1.153	1.286	279.26
0.93	4.067	4.568	17.01	1.447	1.150	1.277	276.04
1.22	4.058	4.555	16.97	1.439	1.145	1.262	272.27
1.50	4.064	4.545	16.96	1.428	1.133	1.248	269.01
1.85	4.084	4.559	17.07	1.415	1.123	1.220	269.08
2.21	4.036	4.528	16.96	1.416	1.129	1.221	263.17
2.66	4.014	4.496	16.95	1.416	1.125	1.223	259.43
3.05	4.001	4.468	17.00	1.416	1.118	1.225	257.17
3.53	3.998	4.435	17.09	1.414	1.105	1.229	254.96
4.00	3.984	4.410	17.10	1.410	1.099	1.229	252.18
4.43	3.970	4.384	17.11	1.407	1.094	1.232	249.51
4.89	3.960	4.364	17.14	1.404	1.089	1.232	247.42
6.05	3.947	4.334	17.12	1.395	1.088	1.224	243.85
6.60	3.945	4.314	17.02	1.397	1.091	1.223	241.57
6.92	3.936	4.305	17.01	1.396	1.091	1.221	240.08
7.52	3.910	4.287	16.97	1.396	1.091	1.222	237.18
8.05	3.886	4.270	16.94	1.394	1.091	1.222	234.27
8.70	3.869	4.257	16.92	1.390	1.088	1.217	231.57

Table 1: Dodecane cell parameters

9 Mechanics of dodecane under pressure

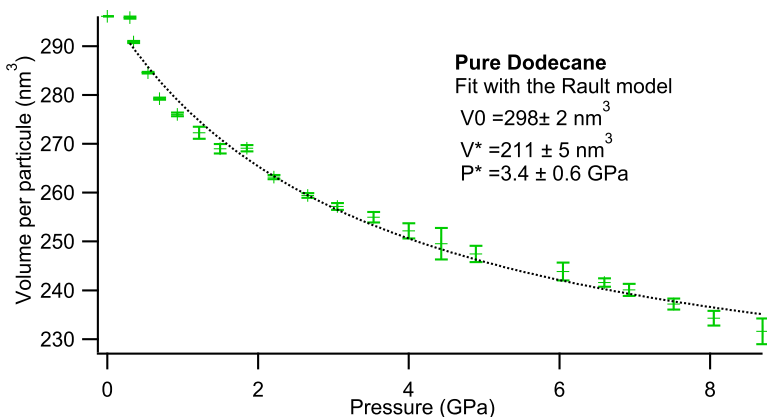


Figure 9: Volume per dodecane particle upon pressure and fit with the Rault's model

10 Behavior of FCC supracrystals at low pressure

To estimate the value of the cell parameter a^* at the transition between the first and the second stage one can estimate the volume V_p occupied by a particle (core plus ligands) at room pressure and assume that the cell parameter is given by $a^{*3} = 4V_p$. The volume fraction occupied by the soft particles is then 100%. The core volume is 61 nm^3 . The number of ligands per particle, assuming a grafting density equal to 5.2 nm^{-2} , is ≈ 10 . The volume per ligand can be estimated to roughly 0.4 nm^3 . The volume per particle (core plus ligand) can thus be estimated to $V_p = 217 \text{ nm}^3$ leading to $a^* = 9.5 \text{ nm}$ in good agreement with the experimental observation. Nevertheless this model is too crude. Indeed since for $a^* = 9.5 \text{ nm}$, there is certainly still some void. In an FCC structure, the particles build octahedral cages. The distance between the cage center and the surface of the surrounding gold cores is $(a^* - D_c)/2 = 2.3 \text{ nm}$, distance that is larger than the extended length of the ligands $L = 1.7 \text{ nm}$. That means that the distribution of the ligands in the soft matrix surrounding the gold cores cannot be considered as a homogeneous medium.